Journal of Alloys and Compounds 510 (2012) 78–82

Contents lists available at SciVerse ScienceDirect

Journal of Alloys and Compounds

journal homepage: www.elsevier.com/locate/jallcom

# First-principles calculations of electronic and optical properties of Ti-doped monoclinic $HfO_2$

Tingting Tan*, Zhengtang Liu, Yanyan Li

*State Key Lab of Solidification Processing, School of Materials Science and Engineering, Northwestern Polytechnical University, Youyixi Road, Xi'an, China*

ARTICLE INFO

*Article history:*
Received 1 August 2011
Accepted 25 August 2011
Available online 3 September 2011

*Keywords:*
Density-functional theory
Electronic structure
Optical properties
Monoclinic $HfO_2$
Ti-doped

ABSTRACT

Based on the first-principles density-functional theory, the electronic structures and optical properties of monoclinic $HfO_2$ and Ti-doped $m$-$HfO_2$ are comparatively investigated. The calculated lattice parameters of $m$-$HfO_2$ are in good agreement with the experimental values and the previous works, and the incorporation of Ti into $HfO_2$ induces a decrease in the lattice parameters. Electronic structures of $m$-$HfO_2$ and Ti-doped $HfO_2$ are studied through the densities of states (DOS) and band structures. The results indicate that the Ti substitution of Hf sites modifies the conduction band structure of $HfO_2$, which leads to a reduction of the band gap of $HfO_2$. The complex dielectric function and refractive index are calculated and the peak position distributions of imaginary parts of the complex dielectric function have been explained. The calculated optical properties are consistent with the experimental measurements for $m$-$HfO_2$.

© 2011 Elsevier B.V. All rights reserved.

## 1. Introduction

In the last decade, hafnium dioxide has been widely studied due to its potential technological applications. $HfO_2$ is characterized by a large dielectric constant, a high melting point, good thermal stability and a wide band gap, and so on [1]. There are several polymorphs in $HfO_2$ which are monoclinic ($m$), tetragonal ($t$) or cubic ($c$) phase, and the orthorhombic phase is observed at high pressure conditions [2]. While $m$-$HfO_2$ is stable at room temperature, the material transforms to a tetragonal structure at 2000 K and to a cubic phase at 2900 K [3]. In its various structures and with the addition of small amounts of impurities, it has been used as the high-$k$ dielectric films [4], optical and protective coatings [5]. More recently, the resistive switching phenomena were observed in the $HfO_2$ thin film [6] and the doped $HfO_2$ films [7].

However, the $k$ value of $HfO_2$ in its most stable monoclinic form does not exceed 25 [8], which limits the application in the continuous device scaling calls for gate dielectric films. Therefore, impurity doping into $HfO_2$ has been studied both experimentally and theoretically in order to improve the dielectric properties. Triyoso et al. [9] investigated the addition of Ti into $HfO_2$ as a means to increase the scalability of $HfO_2$ by increasing the $k$ value of the stack while maintaining the favorable characteristics of $HfO_2$ such as thermal stability, good interface properties and low leakage current. However, the use of Ti or other ions as dopants may impact on other gate stack characteristics. In this respect, Muñoz Ramo et al. [10] have calculated the dielectric response and electron and hole trapping properties of Ti-doped monoclinic $HfO_2$, which showed that the Ti ions serve as deep electron traps inducing localized levels in the Si band gap. In theoretical attempt, the aim of this work is to calculate the electronic structure and optical properties of Ti-doped $HfO_2$, and to find out the probable relations between electronic structure and optical properties using the density functional method.

## 2. Computational method

For our calculations, we employ first-principles methods based on the density functional theory as implemented in the CASTEP code (Cambridge Sequential Total Energy Package) [11]. For the exchange-correlation potential, we employ the localized density approximation (LDA) with the Ceperley–Alder–Perdew–Zunger (CA–PZ) functional [12]. The ionic cores are represented by ultrasoft pseudopotentials for Hf, O and Ti atoms. The Hf (5p, 5d, 6s), O (2s, 2p) and Ti (3s, 3p) levels are treated as valence states.

The plane-wave cutoff energy is 600 eV and the Brillouin-zone integration is performed over the $6 \times 6 \times 6$ grid sizes using the Monkhorst–Pack method [13] for pure $m$-$HfO_2$ structure optimization. The different supercell sizes are used depending on the amount of Ti doping in our calculation. In the geometry optimizations, $2 \times 2 \times 2$ $k$-point grids are employed for the doped $m$-$HfO_2$; the energetic convergence threshold for self-consistent field is $5.0 \times 10^{-6}$ eV/atom; atomic relaxation is carried out until all components of the residual forces are less than 0.1 eV/Å, and the maximum ionic displacement is within $5.0 \times 10^{-4}$ Å.

From the viewpoint of quantum mechanics, the photon absorption or emission has caused transition between the occupied and the unoccupied states, and excitation spectra can be considered as a joint DOS between the valence band and the conduction band [14]. Within the linear response, the macro-optical response function of solid usually can be described by the dielectric function. According to the Kramers–Kronig relationship, the real and imaginary parts of the complex dielectric function can be derived. Then the other optical spectra, such as extinction coeffi-

* Corresponding author.
*E-mail address:* tan-tt@hotmail.com (T. Tan).

0925-8388/$ – see front matter © 2011 Elsevier B.V. All rights reserved.
doi:10.1016/j.jallcom.2011.08.084

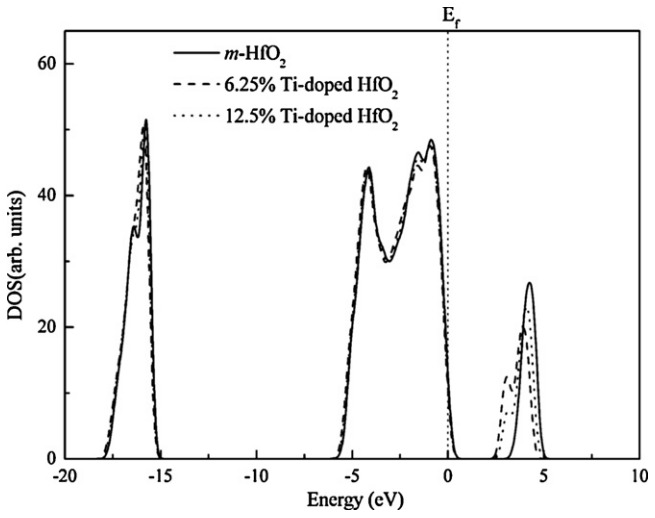


**Fig. 1.** Total density of states for $m$-$HfO_2$ and Ti-doped hafnia. The Fermi level is set to zero.

cient, reflectivity, and refractivity index can be gained by the real part ($\varepsilon_1$) and the imaginary part ($\varepsilon_2$) of the dielectric function [15].

## 3. Results and discussion

### 3.1. Optimized structures

The optimized lattice constants are $a = 5.22$ Å, $b = 5.34$ Å, $c = 5.36$ Å and $\beta = 99.5^\circ$ for pure $m$-$HfO_2$, which are in good agreement with the experimental values ($a = 5.12$ Å, $b = 5.17$ Å, $c = 5.3$ Å, $\beta = 99.2^\circ$) [16]. The calculated values $a = 5.291$ Å, $b = 5.405$ Å, $c = 5.366$ Å, $\beta = 97.92^\circ$ obtained by Zhao and Vanderbilt [17]; $a = 5.189$ Å, $b = 5.241$ Å, $c = 5.344$ Å, $\beta = 99.2^\circ$ computed by Terki et al. [3]. It is clear that our results are in agreement with previous works. The primitive unit cell of $m$-$HfO_2$ (space group $P2_1/c$) contains 12 atoms including four Hf atoms and eight O atoms. The Hf atoms exhibit a sevenfold-coordination, and there are two kinds of oxygen atoms, which have different coordination: $O_1$ having three Hf neighbors and $O_2$ having four Hf neighbors.

The Ti-doped structures are constructed by using the 48-atoms $2 \times 2 \times 1$ and 24-atoms $2 \times 1 \times 1$ supercells with one Hf atom replaced by one Ti atom, which corresponding to 6.25% and 12.5%-doped phases, respectively. The Ti substitution in $m$-$HfO_2$ induces changes in the local lattice structure of the system. In the 6.25% doping case, the Ti–O distances to the three O1 ions decrease by 0.2 Å. Other Ti–O distances remain mostly unaffected. The supercell structure is fully relaxed, and the lattice parameters of the optimized supercells are summarized in Table 1. The results show that there are reductions in the $a$, $b$, $c$ and $\beta$ lattice parameters with the increasing doping concentrations, and the volume of the cell decreases by about 3.5% as doping content increases to 12.5%. The distortions will be useful to the substitution of Ti for Hf in the $m$-$HfO_2$.

### 3.2. Electronic structures

The total electron density of states (DOS) near the Fermi energy of pure $m$-$HfO_2$ and Ti-doped hafnia is presented in Fig. 1. It can be seen that the valence band structure is unaffected by the presence of Ti in the lattice, which is split into two discontinuous groups. The bandwidth of the lower valence band is about 4.0 eV and the peaks of the lower valence band are located at −16.62 eV and −15.87 eV. The bandwidth of the upper valence band is about 7.45 eV includes three peaks at −4.24 eV, −1.68 eV and −1.06 eV, respectively.

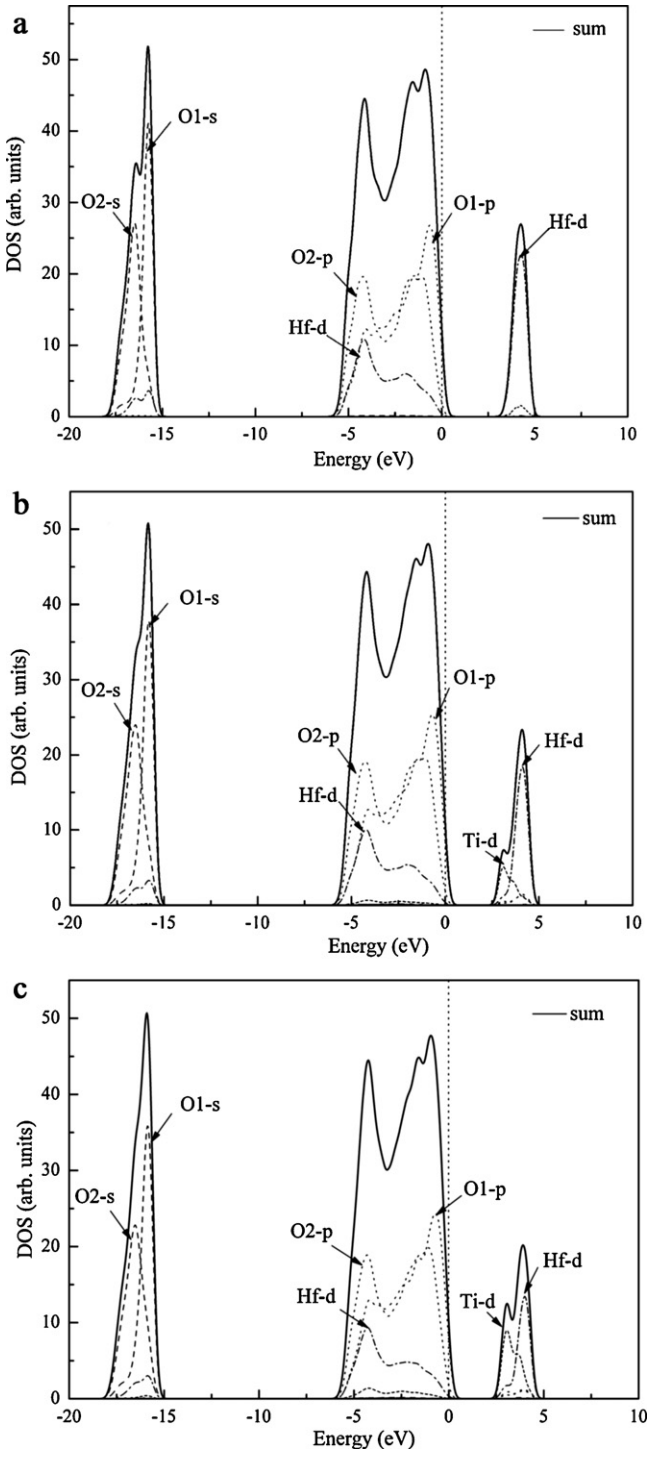


**Fig. 2.** Partial densities of states of Ti-doped $HfO_2$ at different doping levels: (a) 0%, (b) 6.25%, and (c) 12.5%. The Fermi level is set to zero.

For $m$-$HfO_2$, the lower valence band is composed of O 2$s$ states and the upper valence band consists of O 2$p$, which shows a hybridizaiton character with Hf 5$d$. The conduction band is composed mostly of Hf 5$d$ character, and there are a small number of states of O 2$p$ character, as shown in Fig. 2(a). To investigate the doping effect of Ti on the electronic structure of $HfO_2$, the partial DOS are calculated for the Ti-doped hafnia with different doping levels of 6.25 and 12.5%, as shown in Fig. 2(b and c) respectively. The conduction band structure of $HfO_2$ is modified by the incorporation of Ti. A new peak located at about 3.1 eV is induced by Ti 3$d$

**Table 1**
Lattice parameters (in angstrom and degree) and unit-cell volume (in Å$^3$) for monoclinic phase of Ti-doped $HfO_2$ at different doping levels. The *a* and *b* parameters in the Ti-doped phases were obtained by dividing the parameters of the supercells by two.

| Parameter | *a* | *b* | *c* | *α* | *β* | *γ* | Volume |
|---|---|---|---|---|---|---|---|
| 0% | 5.22 | 5.34 | 5.36 | 90.0 | 99.5 | 90.0 | 147.7 |
| 6.25% | 5.19 | 5.33 | 5.32 | 90.1 | 99.3 | 90.1 | 145.2 |
| 12.5% | 5.16 | 5.30 | 5.30 | 90.1 | 99.3 | 90.2 | 142.9 |

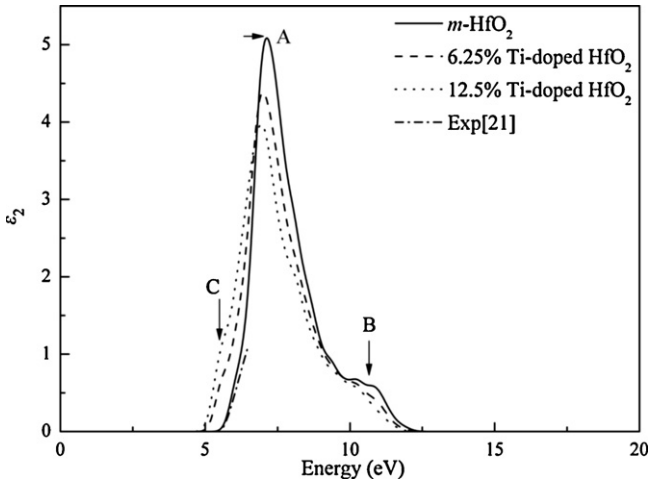


**Fig. 3.** Imaginary parts of the calculated dielectric functions of pure and Ti-doped $m$-$HfO_2$, together with the experimental data [20].

states, which leads to a reduction of the band gap. Therefore one can conclude that the conduction-band offset of Ti-doped $HfO_2$ on Si will decrease with the increasing Ti concentration. In addition, the calculated band structure demonstrates that $m$-$HfO_2$ has indirect band gap, and the band gap is calculated to be about 3.36 eV, which is smaller than the experimental data of 5.68 eV [18] due to the well-known underestimation of conduction band state energies in first-principles calculations.

### 3.3. Optical properties

The complex dielectric function, $\varepsilon(\omega) = \varepsilon_1(\omega) + \varepsilon_2(\omega)$, contains the real $[\varepsilon_1(\omega)]$ and the imaginary $[\varepsilon_2(\omega)]$ parts. The imaginary part $\varepsilon_2(\omega)$ represents the real transitions between the occupied $\psi_k^v$ and the unoccupied $\psi_k^c$ wave functions (electronic states), which is given by [19]:

$$\varepsilon_2(\omega) = \frac{4\pi^2 e^2}{m^2\omega^2 V}\sum_{v,c,k}\left|\left\langle \psi_k^v \left|\vec{P}_i\right| \psi_k^c \right\rangle\right|^2 \delta(E_{\psi_k^c} - E_{\psi_k^v} - \hbar\omega)$$

where $\hbar\omega$ is the energy of the incident photon, $E_{\psi_k^c}$ and $E_{\psi_k^v}$ are the quasi-particle energies, $V$ is the volume of the unit cell, and $\vec{P}_i$ is the momentum operator with $i = x$, $y$ or $z$. Because the calculated band gap of pure $m$-$HfO_2$ (3.36 eV) is smaller than the experimental value (5.68 eV), the scissor operator with the value of 2.32 eV is used for the dielectric function and the related optical properties. Fig. 3 shows the imaginary parts of the calculated dielectric function of pure and Ti-doped $m$-$HfO_2$, together with the experimental values [20]. A good agreement between the calculated values and the experiment values is observed in the range of 0–6.5 eV. For $m$-$HfO_2$, the absorptive part of the imaginary part exhibits two peaks which labeled A and B, respectively. According to the analysis of the

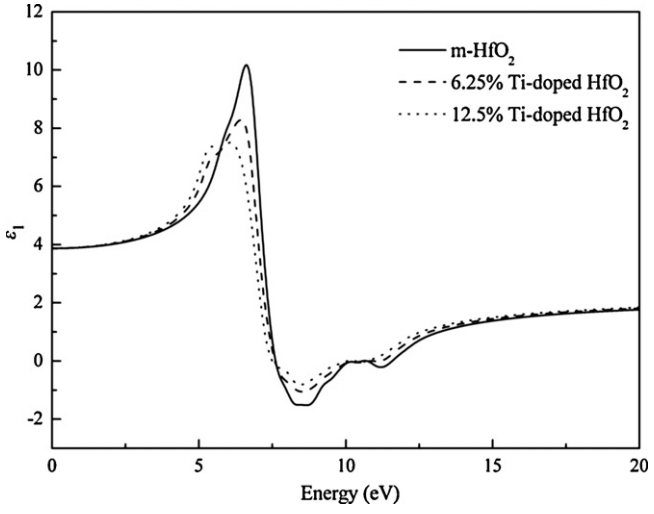


**Fig. 4.** Real parts of the calculated dielectric functions of pure and Ti-doped $m$-$HfO_2$.

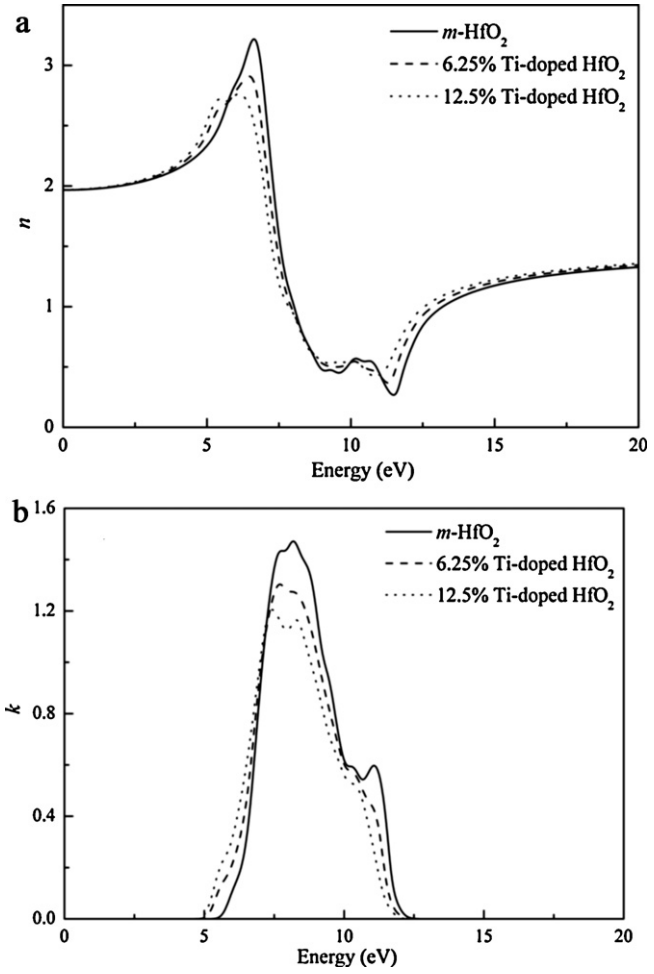


**Fig. 5.** Calculated refractive indexes and extinction coefficients of $m$-$HfO_2$ and Ti-doped $HfO_2$, (a) refractive indexes, and (b) extinction coefficients.

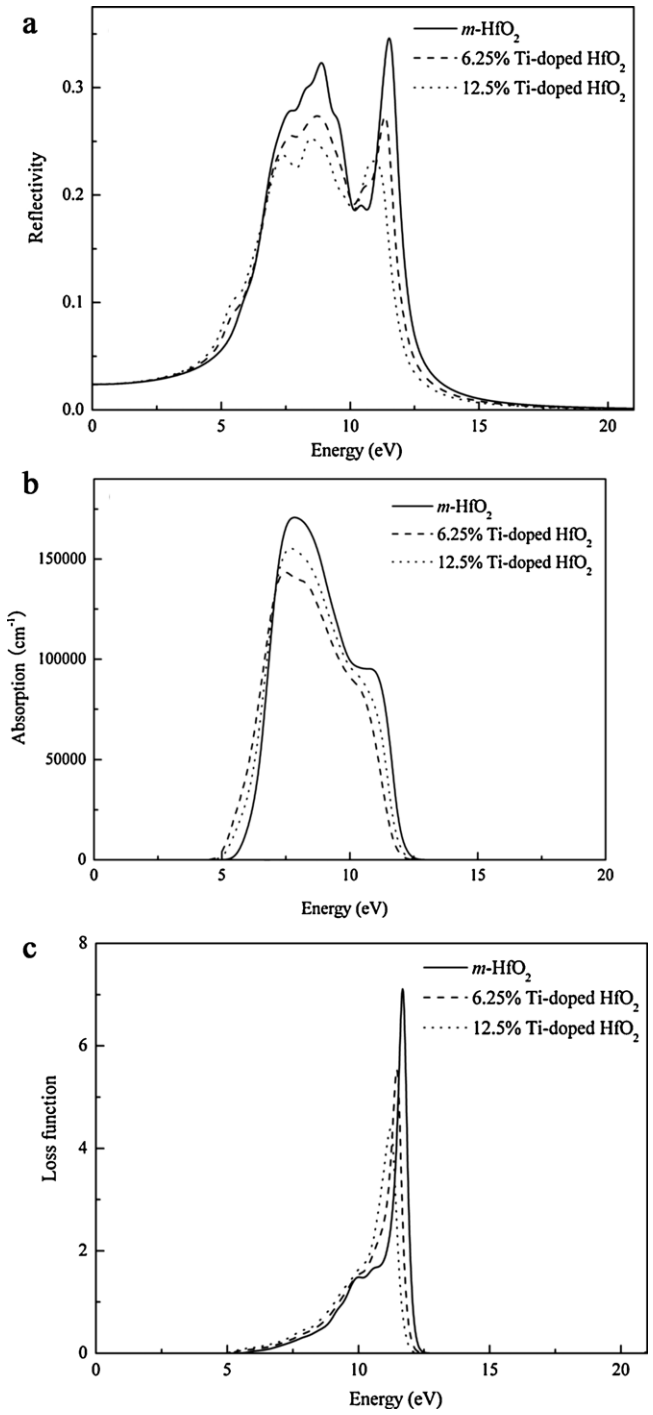


**Fig. 6.** Calculated reflectivity (a), absorption coefficient (b), and loss function (c) of pure and Ti-doped $m$-$HfO_2$.

electronic structure of $m$-$HfO_2$, peak A at 7.13 eV originates from the electronic transition between the O 2p states in the upper valence band and the Hf 5d states in the conduction band. And peak B at 10.16 eV may be due to the transition between the O 2s and the Hf 5d states in the valence band. For 6.25% Ti-doped $HfO_2$, there are three peaks located at 5.53 eV, 7.01 eV and 10.32 eV. The new weak peak C at 5.53 eV may originate from the transition between the O 2p states in the upper valence band and the Ti 3d states in the conduction band. And there are a little position changes of the peaks A and B, which correspond to the localized effects of the Ti ion in the supercell.

The real parts of the calculated dielectric function of $m$-$HfO_2$ and Ti-doped hafnia are presented in Fig. 4. There are mainly two peaks at 6.61 eV and 10.65 eV for the pure $m$-$HfO_2$, and the calculated static dielectric constant of $m$-$HfO_2$ is about 3.87. The calculated results are consistent with the experimental values of Modreanu et al. [21]. Furthermore, the predicted trends of the calculated dielectric functions with increasing energy are in good agreement with Modreanu's results for the monoclinic $HfO_2$ [21]. For the Ti-doped $HfO_2$, there are three peaks of the real parts of the dielectric function corresponding to the imaginary parts. Moreover, the static dielectric constants have no obvious changes compared with pure $m$-$HfO_2$, which is probably due to the low doping levels of Ti ion.

The other optical properties can be calculated from the complex dielectric function $\varepsilon(\omega)$ [22]. The refractive index ($n$) and the extinction coefficient ($k$) of pure and Ti-doped $HfO_2$ are demonstrated in Fig. 5. The static refractive index of $m$-$HfO_2$ is found to be 1.97, which is in good agreement with the experimental value [20]. The reflectivity, absorption, and loss function of the pure and Ti-doped $HfO_2$ systems in the energy range of 0–20 eV are shown in Fig. 6(a–c) respectively. Unfortunately, there are few experimental data for comparison with the calculated results. We hope that the calculated values can help to provide a theoretical basis for the application of doped $HfO_2$. Furthermore, the calculated results may suggest that the incorporation of Ti ion have little influence on the optical properties of $m$-$HfO_2$. However, the addition of Ti ion into hafnia will affect the electrical properties due to the changes in the conduction band structure of $m$-$HfO_2$.

## 4. Conclusion

In conclusion, the electronic structure and the optical properties of pure and Ti-doped $m$-$HfO_2$ are investigated using the first-principles calculations. The lattice parameters of Ti-doped $HfO_2$ are optimized, which are decreasing with increasing doping concentrations. Analysis of the partial DOS of Ti-doped $HfO_2$ indicates that the conduction band structure is modified by the incorporation of Ti ion. The complex dielectric functions and refractive indexes of $m$-$HfO_2$ and doped $HfO_2$ have been predicted. The calculated complex dielectric function and the refractive index of $m$-$HfO_2$ are in good agreement with experimental values. The calculated results indicate that the incorporation of Ti ion mainly has influence on the electronic structure of $m$-$HfO_2$. The results will help to analyze the properties of doped $HfO_2$ and to seek the proper dopants to improve the characteristics of $HfO_2$.

## Acknowledgements

This work was financially supported by the Northwestern Polytechnical University (NPU) Fundamental Research under Grant No. JC201111, the Research Fund of the State Key Laboratory of Solidification Processing (NWPU) under Grant No. 58-TZ-2011, and the 111 Project under Grant No. B08040.

## References

[1] G. He, Q. Fang, G.H. Li, J.P. Zhang, L.D. Zhang, Appl. Surf. Sci. 253 (2007) 8483–8488.
[2] J. Kang, E.-C. Lee, K.J. Chang, Phys. Rev. B 68 (2003) 054106.
[3] R. Terki, G. Bertrand, H. Aourag, C. Coddet, Mater. Lett. 62 (2008) 1484.
[4] M. Liu, L.D. Zhang, G. He, X.J. Wang, M. Fang, J. Appl. Phys. Lett. 108 (2010) 024102.
[5] K. Yamamoto, S. Hayashi, M. Kubota, Appl. Phys. Lett. 81 (2002) 2053.
[6] L. Goux, P. Czarnecki, Y.Y. Chen, L. Pantisano, X.P. Wang, R. Degraeve, B. Govoreanu, M. Jurczak, D.J. Wouters, L. Altimime, Appl. Phys. Lett. 97 (2010) 243509.
[7] Y. Wang, Q. Liu, S.B. Long, W. Wang, Q. Wang, M.H. Zhang, S. Zhang, Y.T. Li, Q.Y. Zuo, J.H. Yang, M. Liu, Nanotechnology 21 (2010) 045202.
[8] G.-M. Rignanese, J. Phys.: Condens. Matter 17 (2005) R357.

[9] D.H. Triyoso, R.I. Hegde, S. Zollner, M.E. Ramon, S. Kalpat, R. Gregory, X.-D. Wang, J. Jiang, M. Raymond, R. Rai, D. Werho, D. Roan, B.E. White Jr., P.J. Tobin, J. Appl. Phys. 98 (2005) 054104.
[10] D. Muñoz Ramo, A.L. Shluger, G. Bersuker, Phys. Rev. B 79 (2009) 035306.
[11] M.D. Segall, P.J.D. Lindan, M.J. Probert, C.J. Pickard, P.J. Hasnip, S.J. Clark, M.C. Payne, J. Phys. Condens. Matter 14 (2002) 2717.
[12] S. Goedecker, M. Teter, J. Huetter, Phys. Rev. B 54 (1996) 1703.
[13] H.J. Monkhorst, J.D. Pack, Phys. Rev. B 13 (1976) 5188.
[14] X.H. Yu, C.S. Li, Y. Ling, T.A. Tang, Q. Wu, J.J. Kong, J. Alloys Compd. 507 (2010) 33.
[15] L.P. Feng, Z.T. Liu, B. Xu, Comput. Mater. Sci. 44 (2009) 929.
[16] J. Wang, H.P. Li, R. Stevens, J. Mater. Sci. 27 (1992) 5397.
[17] X. Zhao, D. Vanderbilt, Phys. Rev. B 65 (2002) 233106.
[18] M. Balog, M. Scheiber, M. Michman, S. Patai, Thin Solid Films 41 (1977) 247.
[19] M. Launay, F. Boucher, P. Moreau, Phys. Rev. B 69 (2004) 035101.
[20] T.T. Tan, Z.T. Liu, H.C. Lu, W.T. Liu, H. Tian, Opt. Mater. 32 (2010) 432.
[21] M. Modreanu, J. Sancho-Parramon, O. Durand, B. Servet, M. Stchakovsky, C. Eypert, Appl. Surf. Sci. 253 (2006) 328.
[22] M.F. Li, Physics of Semiconductor, Science Press, Beijing, 1991.